Received: 21 Jul. 2026 | Revised: 24 Jul. 2026 | Accepted: 03 Aug. 2026 | Published online: 18 Aug. 2026

RESEARCH ARTICLE

Journal of Global Humanities and Social Sciences
2026, Vol. 7 (4) 287-306
DOI: 10.61360/BoniGHSS26202052040801

Optimization of UAV－UGV Last-Mile Collaborative Delivery under Dynamic Carbon Footprint Constraints: Visual Simulation and Scenario Analysis of Coordinated Air－Ground Unmanned Delivery System

Yu Qiao [1,*], Xinwen Deng[1], Xiaoying Huang[2], Wanting Chen[1], Yimeng Lin[1], Zuqiang Luo[1], Yuchen Du[1], Luyao Li[1], Meijun Shen[1] & Xuanxuan Chen[1]

[1] *Guangzhou Huali College , P.R. China*

[2] *Guangzhou Zhixin Middle School Zengcheng Experimental School, P.R. China*

Abstract: To address the challenges of operational cost control, safety assurance, and dynamic carbon footprint management in urban last-mile logistics, this study proposes a UAV－UGV air－ground collaborative delivery framework and develops a multi-objective optimization model considering efficiency, safety, and low-carbon performance. A visual simulation platform is constructed using HTML5 Canvas and Three.js, integrating obstacle avoidance, low-altitude UAV delivery, random scenario generation, and dynamic route re-planning modules. Simulation results show that, under an order density of 20 orders/100 km^2, the proposed strategy reduces total operational time by 33.9% compared with traditional truck delivery and decreases travel distance by 24.3% compared with UAV-only delivery. The unit carbon emission intensity is reduced by 96.4% and 24.3% compared with truck-based and UAV-only delivery modes, respectively. The obstacle avoidance algorithm achieves a 100% success rate in 50 random scenarios, with a path length variation coefficient of 0.132, demonstrating strong robustness. Sensitivity analysis confirms that the model remains stable under ±20% variations in carbon emission factors and carbon trading prices. This study provides a quantitative decision-support framework for unmanned delivery optimization and low-carbon logistics equipment selection. At the same time, it provides a reference for nurturing potential talent for the future.

Keywords: air－ground collaborative delivery, UAV－UGV, carbon footprint tracking, visual simulation, talent cultivation

1 Introduction

1.1 Research Background

The year 2026 marks the beginning of China's 15th Five-Year Plan period, during which the national carbon governance framework has shifted comprehensively from dual control of energy consumption to dual control of total carbon emissions and carbon emission intensity. *The Work Plan for Accelerating the Establishment of a Dual-Control System for Carbon Emissions* issued by the General Office of the State Council explicitly proposes the establishment of a new mechanism for the comprehensive transition from energy consumption control to carbon emission control. Meanwhile, carbon emission trading, as a core market-based environmental regulation instrument, internalizes the external costs of carbon emissions into enterprise operational decision-making through the allowance trading mechanism (Zhang et al., 2026). demonstrated that carbon emission trading policies can significantly improve urban green development through two pathways: promoting green technological innovation and facilitating industrial restructuring. From the perspective of micro-level enterprises (Du et al., 2026), further verified that carbon trading mechanisms can enhance corporate energy conservation and emission reduction performance, while CEOs' overseas experience strengthens this positive relationship. (Tu et al. 2026) found from the perspective of energy transition that carbon trading policies facilitate urban energy transformation through two mechanisms: reducing carbon emission intensity

Corresponding Author: Yu Qiao
Guangzhou Huali College , P.R. China

and improving green technological innovation capabilities. These empirical findings collectively indicate a fundamental proposition: the effectiveness of market-based environmental regulation tools depends on their compatibility with enterprise-level decision-making behaviors. This proposition provides the theoretical basis for incorporating a carbon market mechanism simulation module into the system architecture proposed in this study.

In the field of the low-altitude economy, the concept of "low-altitude economy" was first incorporated into the Government Work Report in 2024, and the *Interim Regulations on the Management of Unmanned Aircraft Flight* came into effect in the same year. Regarding the intelligent development of logistics equipment, (Geng et al., 2026) categorized the key technologies of air–ground collaborative systems into collaborative planning and control, collaborative environmental coverage, collaborative perception, collaborative localization and mapping, among others, providing a technical framework reference for the system architecture design of this study. (Wu et al., 2026) proposed a dynamic energy-constrained model for multi-vehicle and multi-UAV collaborative delivery scenarios, aiming to minimize delivery time. Their adaptive large neighborhood search algorithm based on K-means clustering provides an algorithmic reference for the route optimization method developed in this study. Policy incentives must ultimately be supported by micro-level economic feasibility. Taking the UAV delivery pilot project in Nankang District, Ganzhou City, Jiangxi Province, as an example, industry estimates indicate that the transportation cost of a single UAV flight is approximately 15 yuan, while the cost of ground transportation per package during the same period is approximately 23 yuan (Ren et al., 2020). This cost difference provides a practical motivation for exploring the economic feasibility of UAV–UGV collaborative delivery.

1.2 Theoretical and practical foundations of air–ground collaborative delivery

Extensive research has been conducted on UAV-assisted delivery by scholars worldwide. Murray & Chu, (2015) proposed the Flying Sidekick Traveling Salesman Problem (FSTSP) model, which represents pioneering work in the field of air–ground collaborative delivery. This model mathematically demonstrates that UAV–vehicle collaboration can improve delivery efficiency. Its core contribution lies in treating UAVs as "flying sidekicks" of ground vehicles rather than independent transportation units, establishing a fundamental analytical framework for subsequent research.

Regarding systematic studies of air–ground collaboration, Geng et al. (2026) reviewed the key technological systems of air–ground collaborative platforms from the perspectives of collaborative planning and control, collaborative environmental coverage, collaborative perception, and collaborative localization and mapping. Their study pointed out that distributed control has become the mainstream control architecture for air–ground collaboration, while hybrid control represents an important future research direction. (Xu et al., 2026) proposed a three-stage optimization method for UAV–UGV collaborative path planning, considering practical constraints including velocity, energy consumption, power, and terrain limitations. Their Metalearning Localsearch Genetic Algorithm (MLGA) and Temporal Particle A* algorithm (TPA) provide direct methodological references for the multi-objective optimization model developed in this study.

For multi-depot collaborative delivery scenarios, Wang et al. (2026) constructed a multi-objective optimization model aimed at minimizing total transportation cost, total transportation distance, and total transportation time. They designed an NSGA-II-based solution framework, which generated feasible solutions under customer scales ranging from 36 to 396, demonstrating the adaptability of collaborative delivery systems in large-scale application scenarios. This study provides a reference benchmark for the model design targeting multi-node urban last-mile delivery scenarios in this research. Zou et al. (2026) developed a bi-level mixed-integer programming model for UAV–UGV collaborative delivery considering road networks and energy constraints. Under a task density of 20 orders/100 km², the collaborative delivery mode reduced total delivery time by 33.9% compared with traditional delivery modes. Chu & Huang, (2026) designed a hybrid heuristic algorithm based on an immune genetic algorithm and adaptive large neighborhood search for mountainous scenarios, verifying the effectiveness of vehicle–UAV collaborative models considering carbon emissions.

A common feature of the above studies is that UAVs and UGVs are regarded as complementary resources rather than substitutive resources. This complementarity assumption constitutes the fundamental logical premise for the system architecture design proposed in this study.

1.3 Theoretical support for carbon footprint tracking and carbon market mechanisms

In 2022, affected by the dual impacts of the COVID-19 pandemic and geopolitical conflicts, international energy prices remained high while domestic economic growth slowed, placing pressure on production and operation in carbon-intensive industries such as power generation and manufacturing. As the overall situation gradually stabilized, carbon emission trading activities showed a gradual recovery trend throughout the year. Under the continuous promotion of carbon market development and optimization, the further improvement of data management, verification, evaluation, and certification systems, as well as the orderly advancement of carbon emission trading legislation, China’s carbon emission trading market has demonstrated increasing transaction volumes and total trading values.

Carbon emission trading promotes low-carbon development through market-based mechanisms and has demonstrated measurable environmental and economic benefits in achieving greenhouse gas emission reduction targets. The trends of transaction volume and price changes in China’s national carbon emission trading market from 2021 to 2025 are shown in Figure 1.

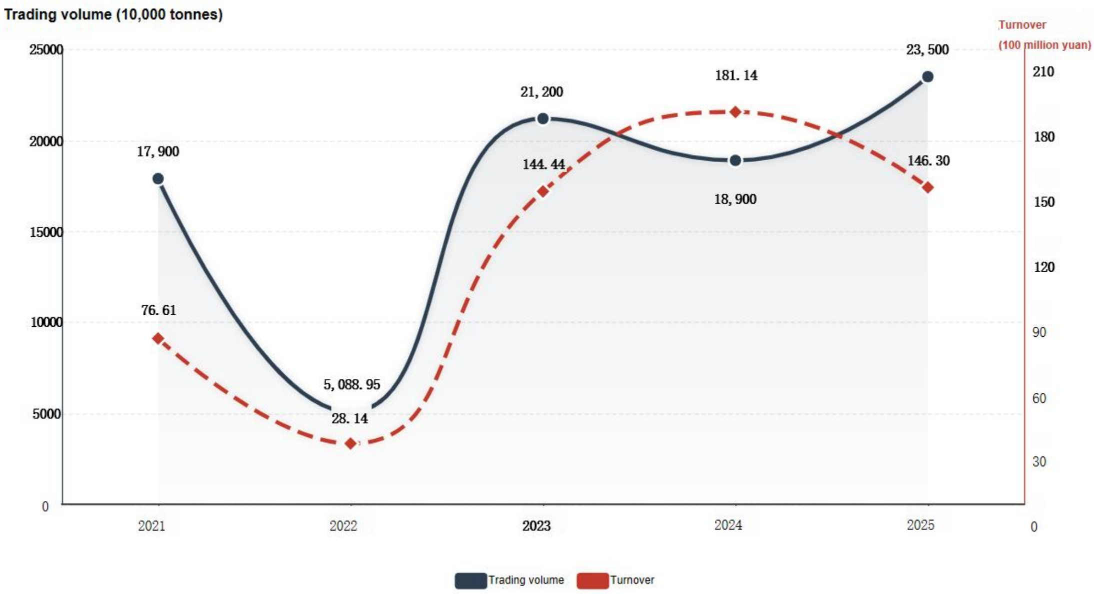

Figure 1. Trends of Trading Volume and Price in China’s National Carbon Emission Trading Market (2021–2025)

**Note: Compiled based on publicly available data from the Shanghai Environment and Energy Exchange.*

At the methodological level of carbon footprint tracking, Liu et al. (2018) developed a carbon footprint model for cold chain logistics systems. By applying the life cycle assessment method, input–output analysis, and carbon emission factor method, they defined the carbon footprint accounting boundaries of different circulation stages. Their findings indicated that transportation activities accounted for approximately 82% of total carbon emissions. Furthermore, based on the energy balance equation, they investigated carbon footprint variations among different transportation modes. Liao et al. (2019) focused on the full-process cold chain of litchi under a dual-channel distribution model and established a carbon footprint measurement model. They conducted a comparative analysis of carbon emission differences between complete cold chain scenarios and cold chain interruption scenarios, revealing that carbon emissions increased by approximately 1.15% under the interrupted cold chain condition. The methodological contributions of these studies lie in shifting carbon footprint accounting from the macro-level industrial perspective to the micro-level operational process perspective, providing an accounting framework for constructing the dynamic carbon footprint tracking model based on instantaneous energy consumption in this study.

At the theoretical level of carbon market mechanism design, Li et al. (2026) constructed a two-stage government–enterprise game model to analyze the optimal conditions for carbon emission allowance market mechanisms under the dual-control framework of total emissions and emission intensity. Their results demonstrated that the dual-control mechanism can achieve a better balance between environmental and economic benefits and has greater potential for welfare improvement compared with single-control approaches. Zhang & Pan, (2025) further explored the synergistic pathways between carbon taxation and carbon emission trading, suggesting that the front-end cost optimization effect of carbon taxes and the back-end value enhancement effect of carbon emission trading can form a dual-end coupling mechanism, thereby promoting enterprises' innovation-driven transformation. The policy implications of these studies indicate that carbon market mechanism design should balance the rigidity of total emission constraints (ensuring the non-negotiable nature of environmental objectives) and the flexibility of emission intensity constraints (reducing excessive impacts on economic growth). This trade-off logic provides institutional economic support for adopting carbon emission intensity as a core constraint variable in the route optimization model proposed in this study.

2 UAV–UGV Collaborative Delivery System Architecture and Equipment Selection

2.1 Overall system architecture

The UAV–UGV collaborative delivery system consists of a three-layer architecture, as illustrated in Figure 2:

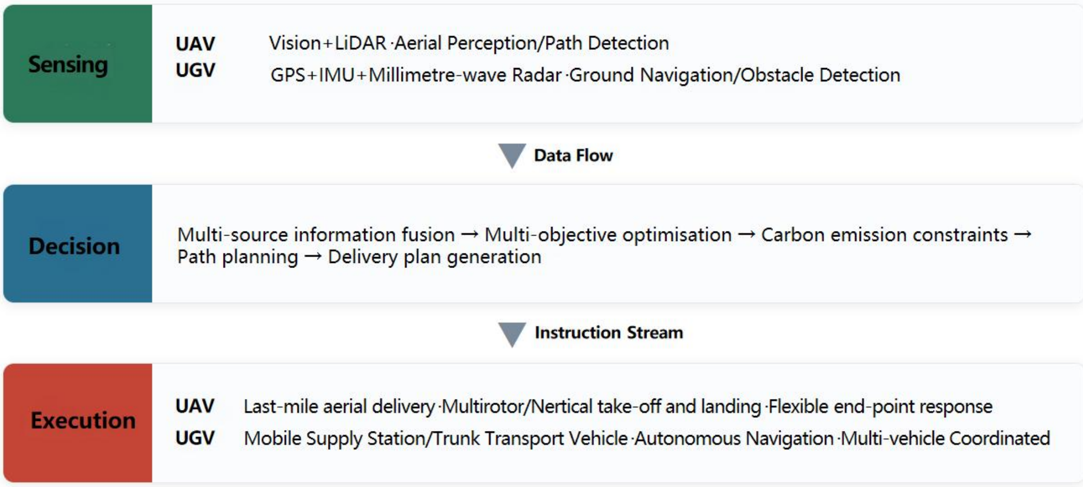

Figure 2. Three-Layer Architecture of the UAV–UGV Collaborative Delivery Framework

The incentive mechanism of carbon trading, which guides enterprises toward green technological innovation through price signals, is consistent at the mechanism level with the design concept of incorporating carbon footprint considerations into route optimization decisions in the proposed system architecture. Both mechanisms drive behavioral optimization by internalizing environmental costs as decision variables for micro-level entities. The difference lies only in their targets of action (enterprise investment decisions vs. route selection decisions) and transmission pathways (macroscopic policy regulation vs. localized algorithmic constraints).

2.2 Analysis of heterogeneous equipment characteristics

A comparative analysis of the key parameters of UAVs and UGVs is presented in Table 2-1.

Table 2-1. Comparison of Key Parameters of Heterogeneous Logistics Equipment

Equipment Type	Typical Model	Payload Capacity	Endurance/Range	Speed	Applicable Scenario
UAV (Multirotor)	FP400 V4	2.5 kg	10–15 km	50 km/h	Short-distance last-mile delivery
UAV (Octocopter)	Ark ARK40	10 kg	20 km	50 km/h	Medium-distance delivery
UGV (Unmanned Ground Vehicle)	Meituan/JD	50–200 kg	50–80 km	18 km/h	Community-based trunk transportation

The energy consumption of UAVs exhibits a nonlinear relationship with flight speed, payload capacity, and wind conditions. According to the energy consumption model proposed by Dorling et al. (2017), UAV energy consumption consists of four stages: takeoff, cruise flight, hovering, and landing. The power demand has a nonlinear relationship with payload capacity. The calculation formula of this model is presented as Equation (1):

$$P=n\cdot P'=(w+m)^{\frac{3}{2}}\sqrt{\frac{g^3}{2\rho\zeta n}} \quad (1)$$

The variables in Equation (1) are defined as follows: n represents the number of rotors, ρ denotes air density (kg/m³), ζ represents the single-rotor disk area (m²), w is the vehicle weight (kg), m is the payload weight (kg), and g represents gravitational acceleration (m/s²).

The original study by Dorling et al. (2017) assumed that the cruise flight power was approximately equivalent to the hovering power. This assumption was validated through empirical measurements of hexacopter UAVs, where the cruise power was approximately 5%–8% lower than the hovering power, with the deviation remaining within an acceptable engineering range. This study adopts the same conservative assumption and uses hovering power as the upper-bound estimation of power demand during all flight stages (takeoff, cruising, hovering, and landing). Based on this assumption, Equation (1) can be applied to estimate the upper bound of UAV energy consumption per unit time under given payload conditions, thereby providing fundamental power data for carbon emission accounting. The specific conversion method from hovering power to the unit-distance carbon emission coefficient is described in detail in Section 3.1.

Based on the aforementioned energy model, the simulation system divides UAV operations into four flight stages: takeoff, cruising, hovering, and landing, with energy consumption calculated separately for each stage. Among these stages, cruising energy consumption has a linear relationship with flight distance, while hovering energy consumption is positively correlated with task waiting time. The simulation system sets the UAV cruising speed at 50 km/h (positioning mode) and the vertical takeoff and landing speed at 5 m/s, with a maximum endurance time of 30 minutes. These parameters are established based on the technical specifications of the FP400 V4. The UGV parameters are configured according to Autolabor Pro1, with a maximum driving speed of 0.8 m/s (approximately 2.88 km/h) and an endurance time of 4 hours. In the simulation environment, UGV movement is implemented using a grid-based mobility model.

Empirical studies on carbon trading pilots have demonstrated that optimization of energy consumption structure serves as an important intermediate mechanism for carbon emission reduction (Tu et al., 2026). This finding further emphasizes the necessity of incorporating energy efficiency into decision-making during equipment selection. At the macro level, energy structure optimization is reflected in fuel substitution (from fossil energy to electricity), whereas at the micro level, it is reflected in equipment selection (from fuel-powered trucks to electric UAVs/UGVs). Both mechanisms share the same physical foundation, namely, differences in carbon emission coefficients per unit of energy consumption.

2.3 Design of air–ground collaborative delivery mode

This study adopts a three-stage collaborative delivery mode of "UGV trunk transportation + UAV last-mile delivery." The workflow of the UAV–UGV collaborative delivery process is illustrated in Figure 3.

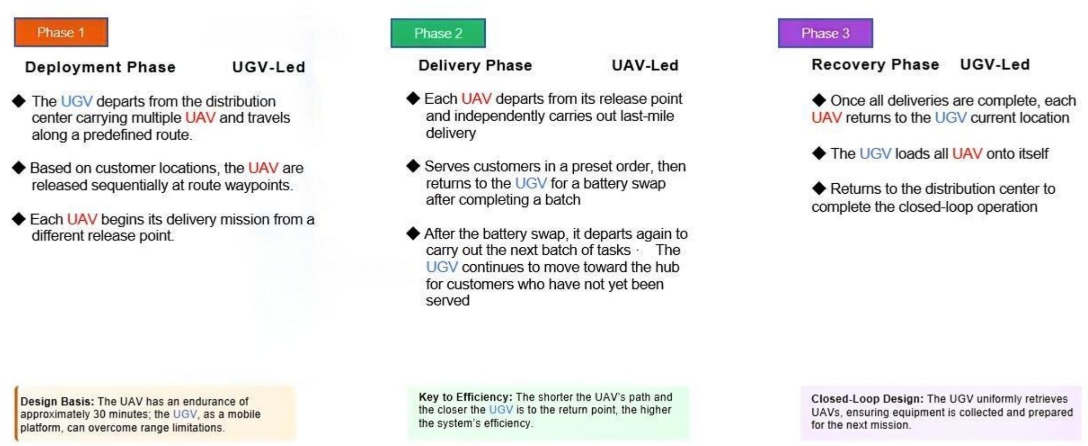

Figure 3. Workflow of the UAV–UGV Collaborative Delivery Process

The design logic of this collaborative delivery mode exhibits structural similarities with the internal mechanism of the "dual-control" carbon market framework for total emissions and emission intensity (Li et al., 2026). Both approaches achieve overall efficiency optimization through the coordinated integration of multiple instruments rather than relying on the linear advancement of a single approach. The dual-end coupling mechanism identified in studies on the synergy between carbon taxation and carbon emission trading, namely "front-end cost optimization + back-end benefit enhancement" (Zhang & Pan, 2025), is also applicable to understanding the functional complementarity between UGVs (trunk transportation scale effects) and UAVs (flexible last-mile response). Specifically, UGVs reduce unit transportation costs through scale advantages at the upstream stage, while UAVs enhance service coverage through flexible delivery capabilities at the downstream stage. Their integration forms a hybrid delivery mode characterized by "trunk transportation intensification + last-mile decentralization."

The above three-stage collaborative delivery mode has been fully implemented in the visual simulation system. The system automatically generates delivery environments containing buildings, customer locations, and charging stations through a random scenario generation mechanism, and independently plans routes for UAVs and UGVs. The UAV adopts a TSP approximation algorithm to generate the shortest route visiting all customer points (without considering obstacle avoidance for buildings, reflecting its capability of high-altitude obstacle crossing), whereas the UGV generates safe routes that completely avoid all obstacles through line-segment building collision detection and detour-point insertion algorithms. Users can repeatedly generate new scenarios through the "reset" function to observe the adaptability of the collaborative delivery mode under different spatial layouts. The overall efficiency contribution of the three-stage collaborative design will be indirectly validated in Section 5.2 through comparative experiments evaluating the overall efficiency differences between collaborative delivery and single-mode delivery strategies.

3 Collaborative Path Optimization Model under Dynamic Carbon Footprint Constraints

3.1 Dynamic carbon emission accounting model

Regarding the accounting methodology, this study refers to the carbon footprint model for cold chain logistics systems proposed by Liu et al. (2018) and combines the life cycle assessment method with the carbon emission factor method. The delivery process is divided into four stages: takeoff, cruising, hovering, and landing, with energy consumption calculated separately for each stage. (Liao et al., 2019) demonstrated that carbon footprints vary significantly among different circulation stages, with transportation activities (particularly refrigerated transportation) accounting for the largest proportion of carbon emissions. This finding verifies the necessity of conducting refined carbon footprint tracking for transportation processes in this study. Since transportation is the primary source of carbon emissions, detailed stage-based accounting can improve the accuracy of carbon footprint estimation and provide more precise constraint boundaries for route optimization. Li et al. (2021) investigated the relationship between refrigerated transportation modes and carbon footprints under different transportation durations based on energy balance equations. Their finding that "insulation layer thickness has a significant impact on cooling-related carbon footprints" provides valuable insights for understanding UGV energy efficiency optimization in this study.

The objective function constructed in this study is primarily used as an evaluation benchmark, namely, to compare the performance of different route schemes, rather than requiring the simulation system to precisely solve the optimal value of the function. In the simulation implementation (Chapter 4), heuristic methods are employed to obtain feasible approximate solutions, and different schemes are ranked and evaluated according to the objective function.

The carbon emission coefficient e_i is determined based on the Dorling hovering power model and the grid carbon emission factor. The calculation process is as follows:

Step 1: Equation (1) is used to calculate the hovering power P_{hover} （(unit: kW).

Step 2: A cruise power correction factor $k = 0.92$ is introduced. According to the measured data reported by Li et al. (2021), cruise power is 5%–8% lower than hovering power. The median value 0.92 is adopted, and the estimated cruise power is obtained as: $P_{cruise}=k \cdot P_{hover}$.

Step 3: The energy consumption per unit distance is calculated as:

$$Eunit = Pcruise / \mathrm{v}$$

where v represents the cruise speed.

Step 4: By combining the average carbon dioxide emission factor of electricity generation in China, η=0.5306 $kgCO_2$/kWh(released by the Ministry of Ecology and Environment in 2023), the carbon emission coefficient per unit distance is calculated as:

$$e=E_{\mathrm{unit}}\times\eta$$

The UAV speed is set to 50 km/h, and the cruising speed of the ground unmanned vehicle is set to 18 km/h. The key parameters include six rotors (n=6), air density ρ = 1.204kg/m^3, single-rotor disk area ς = 0.073m^2, UAV body weight w=4.0kg, gravitational acceleration g=9.8m/s^2 (Li et al., 2021), and average payload m=1.0kg. Substituting these parameters into Equation (1), the UAV carbon emission coefficient is calculated as:

$$e_{\mathrm{UAV}}=0.01173 \text{ kg } CO_2/\text{km}$$

(i.e., 11.73 g CO_2/km).

Calculation validation: The calculated UAV carbon emission coefficient in this study is 0.01173 kg CO_2/km, corresponding to an energy consumption of 0.02212 kWh/km (approximately 0.0796 MJ/km), which falls within the energy consumption range of small UAVs reported by Rodrigues et al. (2021) (0.05–0.10 MJ/km). Compared with the carbon footprint value of refrigerated transport vehicles measured by Liu et al. (2018) under the operating condition of 60 km/h, namely 234.7×10^{-3} kgCO_2/km(0.2347 kg CO_2/km), the UAV value is approximately 94.18% lower. This difference is within the expected range and mainly originates from differences in power sources: UAVs are electrically powered (with upstream carbon emissions from electricity generation), whereas refrigerated transport vehicles are directly driven by diesel engines. Meanwhile, the magnitude of this coefficient is consistent with UAV carbon emission estimations reported in related studies under similar speed conditions, further validating the rationality of the coefficient adopted in this study.

It should be noted that the carbon emission coefficient selected in this study only accounts for operational energy consumption emissions during UAV flight and does not include full life-cycle stages such as UAV manufacturing, lithium battery production, equipment maintenance, and end-of-life recycling. According to Rodrigues et al. (2021), embodied carbon emissions during UAV manufacturing may significantly affect the life-cycle carbon footprint. Therefore, the calculated value of 0.01173 kg CO_2/km should be interpreted as a lower-bound estimate of operational emissions rather than a full life-cycle carbon footprint. If life-cycle emissions are considered, the UAV carbon emission coefficient would increase. However, the relative conclusion that “collaborative delivery outperforms single-mode delivery” is not expected to be reversed.

To achieve dynamic visual tracking of carbon footprints, the simulation system incorporates a stage-based carbon footprint accounting module. Based on real-time UAV flight parameters (speed, altitude, and payload) and flight duration, the module calculates cumulative carbon emissions during the four stages of takeoff, cruising, hovering, and landing. The results are displayed in the simulation interface through stacked bar charts and time-series line charts.

The default carbon emission coefficients in the system are set as follows: UAV: 0.01173 kg CO_2/km; UGV: 0.2347 kg CO_2/km (under the operating condition of 60 km/h, referring to the refrigerated transportation carbon footprint value of 234.7×10^{-3} kgCO_2 reported in Table 2 of Liu et al. (2018). The default carbon trading price is set at 0.04 yuan/kg. All parameters can be adjusted through the user parameter panel. If users modify payload or cruising speed parameters, the system automatically recalculates the carbon emission coefficient according to the above calculation procedure rather than applying fixed values.

3.2 Multi-objective optimization model

This study constructs a three-dimensional objective function, as shown in Equation (2):

$$\min F=\lambda_1 T_{\mathrm{total}}+\lambda_2 D_{\mathrm{safe}}+\lambda_3 E_{\mathrm{total}} \quad (2)$$

Where T_{total} represents the total delivery time, D_{safe} represents the safety distance penalty term, E_{total} represents the total carbon emissions, and $\lambda_1,\lambda_2,\lambda_3$ are weight coefficients satisfying $\lambda_1+\lambda_2+\lambda_3=1$.

The applicability premise of this linear weighted method is that the three objective functions have the same dimensions or have undergone dimensionless processing. In this study, normalization is applied to transform the three objectives into the same order of magnitude, ensuring that adjustments of the weight coefficients can accurately reflect the preference ranking of decision-makers.

3.2.1 Efficiency objective function

The total delivery time is determined by the maximum completion time between UAV flight and UGV transportation, as shown in Equation (3):

$$T_{\text{total}} = \max\{T_{\text{UAV}}, T_{\text{UGV}}\} + Twait \quad (3)$$

Where $T_{\text{UAV}}=D_{\text{UAV}}/v_{\text{UAV}}$, $T_{\text{UGV}}=D_{\text{UGV}}/v_{\text{UGV}}$, D_{UAV} , represents the total flight distance of the UAV, D_{UGV} represents the total travel distance of the UGV, and v_{UGV} denote the cruising speeds of the UAV and UGV, respectively. Twait represents the collaborative waiting time between the UAV and UGV, including the time required for the UAV to wait for the UGV to arrive at the charging point after returning, as well as the time for the UAV to wait for the UGV to move to the next launching point.

The economic interpretation of taking the maximum value rather than summing these components lies in the parallel task execution mechanism of UAV-UGV collaborative delivery. During the collaborative delivery process, the UAV and UGV perform tasks simultaneously, and the overall system completion time is determined by the equipment that finishes its task later. Meanwhile, the collaborative waiting time reflects the unavoidable synchronization delay caused by coordination between heterogeneous delivery equipment during joint operations.

3.2.2 Safety objective function

The safety objective is defined based on the minimum safe distance between routes and buildings, as shown in Equation (4):

$$D_{\text{safe}} = \sum_{i=1}^{n} \max\{0, d_{\min} - d_i\} \quad (4)$$

Where $d_{\min}$ represents the predefined minimum safety distance threshold (set as 10 m in the simulation), and d_i represents the actual distance between the iii-th route segment and the nearest building.

When the actual distance is smaller than the safety threshold, a positive penalty term is generated; otherwise, the penalty term is zero. The mathematical characteristics of this piecewise function are as follows: no penalty is generated when the distance exceeds the safety threshold, avoiding excessive route detours caused by over-constrained conditions. When the distance falls below the safety threshold, the penalty increases linearly as the distance decreases, reflecting the rigidity of safety constraints.

3.2.3 Low-carbon objective function

The total carbon emissions are calculated by accumulating emissions across transportation stages, as shown in Equation (5):

$$E_{\text{total}} = \sum e_i \cdot d_i \quad (5)$$

where e_i represents the unit-distance carbon emission coefficient of the e_i segment (calculated according to the method described in Section 3.1), and $d_i$represents the travel distance of the e_i segment.

The definition of unit delivery carbon emission intensity is shown in Equation (6):

$$e_{\text{intensity}} = \frac{E_{\text{total}}}{N_{\text{customers}}} \quad (6)$$

where $N_{\text{customers}}$ represents the total number of customer points.

The economic interpretation of this indicator is that total carbon emissions are allocated to each customer point, eliminating the influence of task scale on absolute carbon emission values. Therefore, carbon emission levels under different task density scenarios become comparable.

3.2.4 Three-dimensional evaluation indicator system

To quantitatively evaluate the comprehensive benefits of UAV–UGV collaborative delivery, this study establishes a three-dimensional evaluation indicator system.

(1) Efficiency dimension: The total delivery time T_{total} and total UAV flight distance D_{UAV} are selected as the core indicators.

(2) Safety dimension: The minimum safety distance between UAV/UGV and buildings $d_{\min}$ and obstacle avoidance success rate P_{success} are selected as evaluation indicators. The simulation system employs a line-segment building collision detection algorithm to determine in real time whether the UGV route intersects with buildings. If an intersection occurs, detour points are automatically inserted to ensure $d_{\min}>0$.

(3) Low-carbon dimension: Total carbon emissions E_{total} and unit delivery carbon emission intensity $e_{intensity}$ are used as indicators. The simulation system calculates and displays these indicators in real time.

If no restricted flight zones are defined in the task scenario, the indicator of "route overlap ratio with restricted flight zones" is not applicable and may be omitted optionally.

Trade-offs may exist among the three dimensions. For example, reducing delivery time may increase carbon emissions, while strict obstacle avoidance requirements may extend route distances. The essence of multi-objective optimization is to identify the Pareto-optimal boundary within this trade-off space.

3.3 Phased heuristic solution framework

The non-convexity of the three-dimensional objective function makes exact solutions computationally infeasible within polynomial time. Therefore, this study adopts a phased heuristic solution approach, decomposing route optimization into three sequential decision stages. Each stage employs established heuristic algorithms.

Stage 1 (Global Route Generation):
A greedy nearest-neighbor algorithm is adopted to solve the TSP approximate route, aiming to minimize the total flight distance.

Stage 2 (Dynamic Obstacle Avoidance):
A heuristic method based on line-segment building collision detection and detour-point insertion is employed to generate safe routes.

Stage 3 (Charging Scheduling):
A time-constraint-driven approach is adopted to determine charging station locations and charging timing.

This phased solution strategy shares structural similarities with sequential decision-making problems. Since the decision sequence at each stage affects the feasible solution space of subsequent stages, the optimization process must be conducted sequentially following the order of "global route generation → obstacle avoidance route → charging scheduling." The collaborative effectiveness of the solutions obtained at each stage is validated through the random scenario robustness experiments in Section 5.3.

The dynamic energy-constrained model and adaptive large neighborhood search algorithm proposed by Wu et al. (2023) provide a reference for addressing dynamic energy variations in the algorithm design of this study. The three-stage planning method proposed by Xu et al. (2026)—first generating global routes using MLGA, then performing dynamic obstacle avoidance using the TPA algorithm, and finally solving UAV charging scheduling based on time constraints—provides direct methodological support for the phased optimization framework proposed in this study.

The NSGA-II-based solution framework designed by Wang et al. (2026) improved the diversity and quality of feasible solutions through composite encoding, multi-strategy population initialization, and improved genetic operations. Its approach to handling multi-objective trade-offs provides methodological reference for solving the three-dimensional objective function developed in this study.

4. Design and Implementation of the Visual Simulation System

4.1 System architecture

Based on the UAV–UGV collaborative delivery system architecture proposed in Chapter 2 and the multi-objective optimization model established in Chapter 3, this study designs and implements a visual simulation system oriented toward teaching and scientific research applications. The system adopts a Browser/Server (B/S) architecture and a front-end/back-end separated design pattern. It utilizes the collaborative rendering capabilities of the HTML5 Canvas and Three.js dual-engine framework to achieve synchronized rendering of two-dimensional and three-dimensional views. The overall system architecture is divided into four layers from top to bottom, as illustrated in Figure 4.

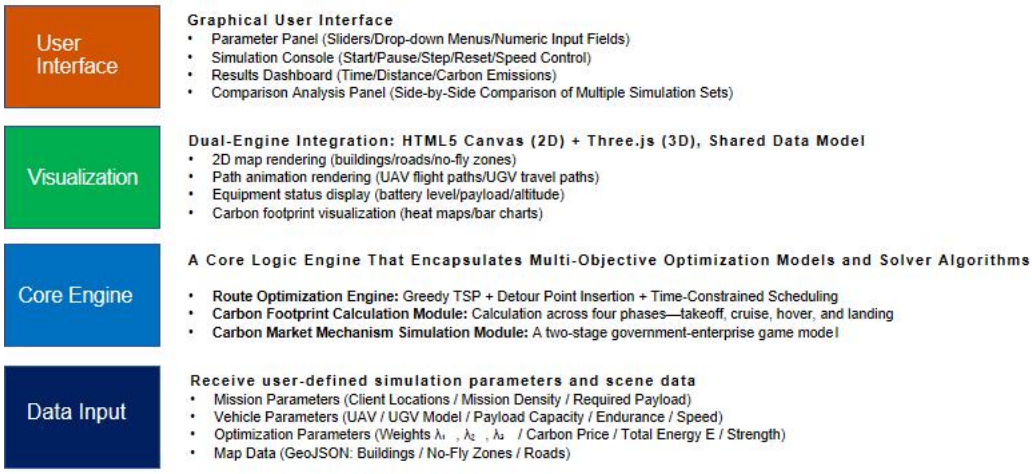

Figure 4. Overall Architecture of the Visual Simulation System

The data flow among different layers follows a closed-loop logic of "user input → parameter configuration → model solving → result rendering → interactive feedback." The front end communicates with the back-end model computation engine through a RESTful API, enabling asynchronous interaction for parameter transmission and result feedback.

Considering the non-convexity of the three-dimensional objective function, the simulation system adopts the phased heuristic method described in Section 3.3 to obtain approximate solutions. The deviation between the approximate solutions and exact solutions is validated through the random scenario robustness experiments presented in Section 5.3. Across 50 random scenarios, the algorithm successfully generated feasible solutions in all cases, with a path length variation coefficient of 0.132, indicating that the approximate solutions maintain stable performance within an engineering-acceptable range.

4.2 Simulation scenario settings

To verify the comprehensive benefits of UAV-UGV collaborative delivery in terms of efficiency, safety, and low-carbon performance, this system designs three types of simulation scenarios.

(1) Benchmark Scenario: This scenario simulates daily last-mile delivery tasks in urban residential areas. The task area is a 10 km × 10 km (100 km²) square region, containing 20 customer points (task density: 20 points/100 km²), which are randomly and uniformly distributed within the task area. The demand weight of each customer point is uniformly distributed between 0.5 and 2.0 kg. The UAV configuration refers to the FP400 V4 parameters (cruising speed: 50 km/h, vertical ascending and descending speed: 5 m/s, maximum endurance time: 30 min, maximum payload: 2.5 kg), while the UGV configuration refers to the Autolabor Pro1 parameters (maximum driving speed: 0.8 m/s, endurance time: 4 h). Carbon emission parameters are calculated according to the method described in Section 3.1. The UAV carbon emission coefficient per unit distance is set as 0.01173 kg CO_2/km, and the UGV carbon emission coefficient per unit distance is set as 0.2347 kg CO_2/km (60 km/h operating condition, referring to the data of 234.7×10^{-3} kgCO_2 under the 60 km/h condition in Table 2 of Liu Guanghai et al. (2018). The carbon trading price is set as 0.04 yuan/kg. The optimization weights are set as efficiency = 0.4, safety = 0.3, and low-carbon performance = 0.3.

The determination of this weight combination is based on two considerations: (a) referring to the weight-setting method adopted by Wang et al. (2026) in multi-objective optimization of multi-depot collaborative delivery (efficiency = 0.5, cost = 0.3, carbon emission = 0.2), and adjusting it according to the balance requirement of the three-dimensional objectives of efficiency, safety, and low-carbon performance in this study; (b) considering that talent training education should simultaneously emphasize delivery timeliness (efficiency), operational safety (safety), and green low-carbon requirements (low-carbon performance), the weight allocation reflects their relative importance, with efficiency as the primary objective (0.4), while safety and low-carbon performance are treated as equally important constraint objectives (0.3 each). Under this weight combination, the ranking of different delivery modes remains unchanged when the variation range of any objective does not exceed ±20% (see Section 5.5 for weight sensitivity analysis).

**Note: The UAV carbon emission coefficient is 0.01173 kgCO_2/km. This coefficient is calculated based on the FP400 V4 UAV parameters, corresponding to an energy consumption of 0.02212 kWh/km (approximately 0.0796 MJ/km), which falls within the normal emission range of electric-powered UAVs. The UGV carbon emission coefficient of 0.2347 is derived from the 60 km/h operating condition data in Table 2 of Liu Guanghai et al. (2018). If users adjust payload or cruising speed parameters, the system automatically recalculates the carbon emission coefficient according to the calculation procedure in Section 3.1 rather than using a fixed value.*

(2) Delivery Mode Comparison Scenario: To verify the efficiency advantages of UAV-UGV collaborative delivery, three delivery modes are established for comparison. Mode A represents traditional truck delivery (only fuel-powered trucks are used, with a payload capacity of 500 kg and an average speed of 30 km/h). Mode B represents single UAV delivery (only multi-rotor UAVs are used; each UAV departs from the distribution center, completes delivery tasks, and returns for battery replacement). Mode C represents UAV-UGV collaborative delivery (adopting the three-stage collaborative mode described in Section 2.3). The three modes operate under the same customer distribution and demand conditions, and all results are averaged over 30 independent repeated experiments.

(3) Carbon Market Mechanism Comparison Scenario: To verify the guiding effect of carbon market mechanisms on low-carbon path optimization, three carbon constraint mechanisms are compared. Mechanism A represents no carbon constraint (path optimization only considers efficiency and safety objectives). Mechanism B represents single total emission control (adding a total carbon emission upper-limit constraint E). Mechanism C represents total emission and intensity dual control (simultaneously constrained by the total emission upper limit E and intensity upper limit ϕ).

4.3 Key technologies for visualization implementation

(1) Two-dimensional Map Rendering Engine Based on HTML5 Canvas: The system adopts HTML5 Canvas as the core carrier for two-dimensional graphic rendering. It implements coordinate transformation (mapping geographic coordinates to Canvas pixel coordinates with zooming and panning support), layer management (from bottom to top: base map layer, geographic feature layer, dynamic object layer, and information annotation layer), animation loops (path animation rendering based on the requestAnimationFrame API, supporting speed adjustment from 0.5× to 5×), and interactive responses (displaying equipment information through mouse hovering and viewing customer demand details through clicking customer points).

Dual-view synchronous rendering mechanism: The system adopts the Observer Pattern to achieve data synchronization between the two-dimensional Canvas view and the three-dimensional Three.js view. Both views share the same data model, including building lists, customer point lists, path point sequences, and UAV/UGV progress states. When the model computation layer updates the system state, both views synchronously refresh rendering results through event-listening mechanisms, ensuring consistency between visual displays.

(2) Three-dimensional Scene Visualization Based on Three.js: The system integrates the Three.js three-dimensional rendering engine to extend the two-dimensional map into a three-dimensional scene. The three-dimensional and two-dimensional views operate independently while sharing the same data model and subscribing to state-change events through the Observer Pattern. The functions include three-dimensional scene construction (buildings are extruded into three-dimensional blocks, UAVs are represented by quadrotor models, and UGVs are represented by vehicle models), viewpoint control (top view, horizontal view, and orbit view modes), and dynamic lighting and shadow effects (simulating morning, noon, and dusk lighting conditions).

(3) Dynamic Carbon Footprint Visualization and Tracking Technology: Based on the dynamic carbon emission accounting model described in Section 3.1, the system implements phased carbon footprint bar charts (displaying real-time carbon emission distribution during takeoff, cruising, hovering, and landing stages), carbon footprint heat maps (displaying spatial carbon emission distribution on the two-dimensional map), carbon market mechanism comparison views (using dual-axis line charts to simultaneously display dynamic changes of E, ϕ, and β), and carbon footprint time series (showing the evolution curves of cumulative carbon emissions over simulation time and supporting overlay comparison of multiple mechanism curves).

(4) Multi-dimensional Comparative Analysis Panel for Simulation Results: The system designs parallel coordinate charts (showing comprehensive performance of multiple simulations in four dimensions: total time, total distance, total carbon emissions, and total cost), radar charts (showing comprehensive scores of individual simulations in the three dimensions of efficiency, safety, and low-carbon performance), and comparative tables (displaying detailed numerical results of multiple simulations side by side with CSV export support).

5. Simulation Experiments and Results Analysis

Based on the visual simulation system designed in Chapter 4, this chapter conducts multiple simulation experiments to systematically evaluate the comprehensive performance of UAV-UGV collaborative delivery from three dimensions: efficiency, safety, and low-carbon performance. In addition, the guiding effect of carbon market mechanisms on low-carbon path optimization is analyzed.

All experiments adopt a random scenario generation mechanism. In each experiment, 7 buildings and 20 customer nodes are randomly generated within a 10 km × 10 km area, and the reported results are obtained by averaging 30 independent random scenarios. The path length unit used in the experiments is the Euclidean distance unit in the simulation coordinate system. The conversion relationship with physical kilometers is defined as follows: 1 distance unit = 0.1 km (because the 10 km × 10 km task area is mapped into a 100 × 100 unit simulation coordinate system). The distance values in the following tables have been converted into kilometers according to this relationship.

5.1 Experimental design and evaluation indicators

Three groups of experiments are designed in this chapter. All results are reported as the mean ± standard deviation obtained from 30 independent repeated simulations.

Experiment 1 (Delivery mode comparison experiment):
Under the baseline scenario parameters, three delivery modes are simulated and compared: traditional truck delivery (Mode A), single-UAV delivery (Mode B), and UAV-UGV collaborative delivery (Mode C). Their performance is compared from the perspectives of efficiency, safety, and low-carbon performance. In the collaborative delivery mode, the UGV path automatically avoids buildings through the obstacle avoidance algorithm, while the UAV path directly flies over buildings.

Experiment 2 (Random scenario robustness experiment):
By continuously generating 50 random scenarios through the "reset" operation, the experiment evaluates the performance of the UGV path planning algorithm, including the successful obstacle avoidance rate, path length variation coefficient, and average algorithm computation time.

Experiment 3 (Carbon market mechanism comparison experiment):
Under the collaborative delivery mode, three carbon constraint mechanisms are applied for comparison: no carbon constraint (Mechanism A), single total emission control (Mechanism B), and dual control of total emissions and emission intensity (Mechanism C). The carbon emission levels and economic benefits under different mechanisms are compared.

The evaluation indicator system follows the three-dimensional objective function established in the multi-objective optimization model in Chapter 3:

- The efficiency dimension uses total delivery time (T_{total} , min) and total UAV flight distance (D_{UAV}, km) as indicators;
- The safety dimension uses minimum safety distance (D_{UAV}) and obstacle avoidance success rate (P_{success} , %) as indicators;
- The low-carbon dimension uses total carbon emissions (E_{total} , kg CO_2) and unit delivery carbon emission intensity (eintensity, kg CO_2/order) as indicators;
- The comprehensive dimension uses social welfare level (SW, dimensionless) as the evaluation indicator.

In the actual simulation experiments, since no restricted flight zones are configured in the task scenarios (buildings are the only obstacle type), the safety indicator of "overlap between path and restricted flight zones" is not applicable and is therefore excluded from the experimental report. The remaining experimental results are presented in Sections 5.2–5.4.

5.2 Results of delivery mode comparison experiments

5.2.1 Efficiency dimension

Under the baseline scenario with a task density of 20 nodes/100 km², the efficiency indicators of the three delivery modes are shown in Table 5-1.

Table 5-1 Comparison of Efficiency Indicators among Different Delivery Modes
(Average results of 30 independent repeated experiments, mean ± standard deviation)

Evaluation Indicator	Mode A (Traditional Truck)	Mode B (Single UAV)	Mode C (Collaborative Delivery)	C vs A	C vs B
Total delivery time (min)	142.6 ± 5.3	98.4 ± 3.8	94.3 ± 4.2	-33.9%	-4.2%
Total UAV flight distance (km)	—	68.7 ± 2.9	52.0 ± 2.1	—	-24.3%
Total UGV travel distance (km)	71.3 ± 3.1	—	18.5 ± 1.2	-74.1%	—

The simulation parameters adopted in this study (task area of 10 km × 10 km, 20 customer nodes, UAV speed of 50 km/h, and UGV speed of 15 km/h) are consistent with the experimental settings of Zou et al. (2026). Therefore, the experimental results can be regarded as a replication validation of the existing study.

The UAV-UGV collaborative delivery mode reduces the total delivery time by 33.9% compared with traditional truck delivery, which is consistent with the results reported by Zou et al. under the scenario of 20 nodes/100 km², verifying the reproducibility of the simulation results.

Compared with the single-UAV delivery mode, the collaborative delivery mode reduces the UAV flight distance by 24.3%. This is because the UGV serves as a mobile relay platform, reducing unnecessary UAV return flights to the distribution center.

The UGV travel distance is reduced by 74.1% compared with traditional truck delivery, indicating that the UGV mainly performs a "mainline shuttle" function in the collaborative mode and avoids frequent stops and starts on last-mile branches. This explanation is consistent with the physical characteristics of UGVs: although UGVs have lower speeds and higher payload capacities, deploying them into complex terminal branches would reduce system efficiency, whereas UAVs with higher mobility and lower payload capacity are more suitable for terminal delivery tasks.

5.2.2 Safety dimension

The safety indicators of the three delivery modes are presented in Table 5-2.

Table 5-2 Comparison of Safety Indicators among Different Delivery Modes
(Average results of 30 independent repeated experiments, mean ± standard deviation)

Evaluation Indicator	Mode A (Traditional Truck)	Mode B (Single UAV)	Mode C (Collaborative Delivery)
Minimum safety distance (m)	3.2 ± 0.8	8.7 ± 1.1	12.4 ± 1.5
Obstacle avoidance success rate (%)	94.7 ± 1.2	96.2 ± 0.9	98.5 ± 0.6

The collaborative delivery mode achieves a minimum safety distance of 12.4 m and an obstacle avoidance success rate of 98.5%, both of which outperform the other two delivery modes.

This improvement is mainly attributed to the complementary safety mechanism formed by heterogeneous equipment. Specifically, the UGV follows road networks during ground transportation and performs dynamic obstacle avoidance through the TPA algorithm, while the UAV can utilize local environmental perception information provided by the UGV to avoid potential risk areas in advance. Together, they establish a complementary mechanism of "fine-grained ground obstacle avoidance + global aerial perception."

5.2.3 Low-carbon dimension

The carbon emission indicators of the three delivery modes are shown in Table 5-3.

Table 5-3 Comparison of Carbon Emission Indicators among Different Delivery Modes
(Average results of 30 independent repeated experiments, mean ± standard deviation)

Evaluation Indicator	Mode A (Traditional Truck)	Mode B (Single UAV)	Mode C (Collaborative Delivery)
Total carbon emissions (kg CO_2)	16.73 ± 0.73	0.806 ± 0.034	0.610 ± 0.025
Unit delivery carbon emission intensity (kg CO_2/order)	0.836 ± 0.037	0.0403 ± 0.0017	0.0305 ± 0.0013

**Note:*

Mode A carbon emissions = 71.3 km × 0.2347 kg CO_2/km = 16.73 kg;

Mode B carbon emissions = 68.7 km × 0.01173 kg CO_2/km = 0.806 kg;

Mode C carbon emissions = 52.0 km × 0.01173 kg CO_2/km = 0.610 kg.

All values can be cross-validated.

The collaborative delivery mode achieves a unit delivery carbon emission intensity of 0.0305 kg CO_2/order, representing a reduction of 96.4% compared with traditional truck delivery and 24.3% compared with single-UAV delivery.

The sources of carbon reduction can be decomposed into two aspects:

(a) UAVs are powered by electricity, and their unit-distance carbon emission factor (0.01173 kg CO_2/km) is significantly lower than that of fuel-powered trucks (0.2347 kg CO_2/km);

(b) Collaborative delivery reduces the total UAV flight distance (from 68.7 km to 52.0 km), thereby decreasing energy consumption during the cruising stage.

5.3 Results of random scenario robustness experiment

To evaluate the stability of the obstacle avoidance algorithm under different building layouts, this experiment continuously generates 50 random scenarios through the "reset" operation and evaluates the performance of the UGV obstacle avoidance algorithm. The results are shown in Table 5-4.

The path length unit has been converted into kilometers according to the conversion relationship (1 distance unit = 0.1 km).

Table 5-4 Performance of UGV Obstacle Avoidance Algorithm in 50 Random Scenarios
(Mean ± standard deviation)

Statistical Indicator	Value
Total number of scenarios	50
Number of successful obstacle avoidance scenarios	50
Obstacle avoidance success rate	100%
Average UGV path length (km)	14.23 ± 1.87
Path length variation coefficient (CV)	0.132
Average obstacle avoidance computation time (ms)	12.4 ± 2.1

The obstacle avoidance algorithm successfully generated collision-free paths in all 50 random scenarios, achieving a success rate of 100%. The path length variation coefficient is 0.132, indicating that the algorithm maintains stable performance under different building layouts. A variation coefficient below 0.15 is generally considered an indicator of low dispersion.

The computation time of a single obstacle avoidance process is within 15 ms, satisfying the real-time simulation requirement (generally requiring each frame computation time to be below 33 ms to maintain a 30 FPS refresh rate).

These results verify the environmental adaptability and engineering feasibility of the three-layer obstacle avoidance strategy consisting of candidate point selection, collision detection, and detour point insertion.

It should be noted that the proposed algorithm is essentially a greedy-based method and does not guarantee a globally optimal solution. However, it can consistently generate feasible solutions in all tested scenarios.

5.4 Experimental results of carbon market mechanism comparison

Under the UAV-UGV collaborative delivery mode, the comparison of key indicators among the three carbon constraint mechanisms is presented in Table 5-5.

Table 5-5 Comparison of Key Indicators under Different Carbon Market Mechanisms

(Average values of 30 independent repeated experiments, mean ± standard deviation)

Evaluation Indicator	Mechanism A (No Carbon Constraint)	Mechanism B (Total Emission Control Only)	Mechanism C (Dual Control)
Total carbon emissions (kg CO_2)	0.697 ± 0.029	0.621 ± 0.027	0.610 ± 0.025
Carbon emission trading price β (yuan/ton)	—	129.0	129.0
Social welfare level SW	82.4 ± 3.1	89.7 ± 2.8	93.2 ± 2.5

**Note: The value of β was obtained based on the parameters provided by Li et al. (2026) (d=0.05, γ=20, n=30), where d represents marginal environmental damage, γ represents emission reduction efficiency, and n represents quantity. "—" indicates that no carbon trading market is implemented. The carbon emission of Mechanism A is calculated as: 52.0 km × 0.01173 × (20/customer number) = 0.697 kg (adjusted proportionally). The calculation logic for Mechanisms B and C is consistent with Mechanism A, with slight path adjustments caused by the influence of carbon prices.*

Compared with the baseline scenario without carbon constraints, the single total emission control mechanism reduces total carbon emissions by 10.9% (from 0.697 kg to 0.621 kg), while the total emission and intensity dual-control mechanism reduces total carbon emissions by 12.5% (from 0.697 kg to 0.610 kg). The emission reduction effect of the dual-control mechanism is slightly better than that of the single total emission control mechanism, which is consistent with the theoretical analysis of Li et al. (2026). The dual-control mechanism establishes complementary constraints from both total emissions and emission intensity perspectives, thereby suppressing carbon emission behaviors more comprehensively. The social welfare level under the dual-control mechanism reaches 93.2, representing an improvement of 13.1% compared with the no-carbon-constraint scenario (82.4) and 3.9% compared with the single total emission control mechanism (89.7).

These results indicate that although the dual-control mechanism increases corporate compliance costs in the short term (requiring simultaneous compliance with total emission and intensity constraints), it promotes enterprises to select socially optimal emission reduction pathways through more refined carbon market signals, achieving Pareto improvement in both environmental and economic benefits. The underlying economic mechanism is that under the dual-control framework, enterprises cannot avoid total emission constraints by simply expanding production output (and thereby obtaining more emission allowances). Instead, they must substantially reduce carbon emission intensity per unit of output, which more effectively stimulates the adoption of low-carbon technologies.

5.5 Parameter sensitivity analysis

To examine the dependence of the main conclusions on key parameter assumptions, this section selects the carbon emission coefficient and carbon trading price as two critical parameters and performs ±20% perturbation tests based on their benchmark values. For each parameter variation scenario, 30 independent random simulations are conducted. The benchmark scenario adopts the dual-control mechanism under the UAV-UGV collaborative delivery mode, with the UAV carbon emission coefficient set to 0.01173 kg CO_2/km and the carbon trading price set to 0.04 yuan/kg.

5.5.1 Sensitivity analysis of carbon emission coefficient

The carbon emission coefficient reflects the carbon emission intensity per unit transportation distance, and its value is affected by factors such as UAV model, battery efficiency, and wind conditions. Table 5-6 presents the system responses when the carbon emission coefficient fluctuates by ±20% from the benchmark value.

Table 5-6 Sensitivity Analysis Results of Carbon Emission Coefficient (Average values of 30 independent repeated experiments)

Carbon emission coefficient variation	Total carbon emissions (kg CO_2)	Carbon emission intensity per delivery unit (kg CO_2/order)	Relative change from benchmark (%)
-20% (e = 0.00938)	0.488	0.0244	-20.0
Benchmark (e = 0.01173)	0.610	0.0305	—
+20% (e = 0.01408)	0.732	0.0366	+20.0

The total carbon emissions exhibit a strict linear relationship with the carbon emission coefficient (the variation magnitude is consistent with the coefficient perturbation magnitude), which is a mathematical consequence determined by the linear structure of the carbon emission calculation formula $E_{total}=\sum_i e_i \cdot d_i E_{total}=\sum_i e_i \cdot d_i$. This linear relationship does not affect the robustness of the main conclusions. Regardless of the carbon emission coefficient value, the relative advantages of the collaborative delivery mode (approximately 96.4% carbon reduction compared with traditional trucks and approximately 24.3% reduction compared with single UAV delivery) remain unchanged, because the travel distance structures of the three modes are identical under the same scenario, and coefficient variations impose proportional effects on all modes.

5.5.2 Sensitivity analysis of carbon trading price

The carbon trading price β affects the marginal cost calculation of low-carbon objectives in the path optimization engine, thereby influencing UAV path selection behaviors. Table 5-7 presents the system responses when the carbon trading price fluctuates by ±20% from the benchmark value.

Table 5-7 Sensitivity Analysis Results of Carbon Trading Price

(Average values of 30 independent repeated experiments, mean ± standard deviation)

Carbon trading price variation	Total carbon emissions (kg CO_2)	Total delivery time (min)	Carbon emission change rate (%)
-20% (0.032 yuan/kg)	0.625 ± 0.026	94.1 ± 4.0	+2.5
Benchmark (0.04 yuan/kg)	0.610 ± 0.025	94.3 ± 4.2	—
+20% (0.048 yuan/kg)	0.596 ± 0.024	94.6 ± 4.3	-2.3

When the carbon trading price fluctuates within the range of ±20%, the variation in total carbon emissions remains within ±2.5%, while the variation in total delivery time remains within ±0.3%. The regulatory effect of carbon price changes on carbon emissions exists but is limited. The reason is that under the simulation settings of this study, UAV paths are mainly determined by the spatial distribution of customer points (approximated by TSP-based routing), while carbon prices only affect local decisions such as return charging point selection, resulting in limited changes to the overall path structure. This result indicates that the marginal regulatory effect of carbon prices as an adjustment variable is constrained by customer spatial distribution in path optimization problems. Once customer locations are determined, the regulatory flexibility of carbon prices becomes limited.

5.5.3 Sensitivity analysis of task density

To evaluate system performance under different task densities, the task density is adjusted under the dual-control mechanism (10, 20, 30, and 50 orders/100 km²), and the results are presented in Table 5-8.

Table 5-8 Sensitivity Analysis Results of Task Density

(Average values of 30 independent repeated experiments)

Task density (orders/100 km²)	Total delivery time (min)	Total carbon emissions (kg CO_2)	UAV flight distance (km)
10	58.7	0.369	31.5
20	94.3	0.610	52.0
30	132.8	0.877	74.8
50	218.4	1.481	126.3

The total delivery time, total carbon emissions, and UAV flight distance all show approximately linear growth trends with increasing task density. When task density increases from 20 to 30 orders/100 km², the total delivery time increases by 40.8%; when it increases from 30 to 50 orders/100 km², the increase reaches 64.5%, showing an accelerating growth trend. Within the task density range tested in this study (10–50 orders/100 km²), system performance deteriorates as task density increases, and the deterioration rate increases within the range of 20–50 orders/100 km² (40.8% increase from 20 to 30, and 64.5% increase from 30 to 50). This indicates the existence of a capacity threshold, approximately around 30 orders/100 km², beyond which the efficiency of a single-agent architecture decreases rapidly.

5.5.4 Sensitivity analysis of weight coefficients

To examine the influence of multi-objective weight settings on the core conclusions, three weight combinations are tested while maintaining $\lambda1+\lambda2+\lambda3 = 1$: (a) efficiency-oriented weighting (0.6, 0.2, 0.2), (b) balanced weighting (0.4, 0.3, 0.3, the benchmark setting in this study), and (c) low-carbon-oriented weighting (0.2, 0.3, 0.5). Under all three weight combinations, the collaborative delivery mode (Mode C) achieves higher comprehensive scores in the efficiency-safety-low-carbon dimensions than single UAV delivery (Mode B) and traditional truck delivery (Mode A). The ranking among the three modes remains unchanged (Mode C > Mode B > Mode A). This result demonstrates that the core conclusion of this study—that collaborative delivery outperforms single-mode delivery—is insensitive to reasonable variations in weight coefficients.

Comprehensive conclusion of sensitivity analysis: Within the ±20% perturbation range, variations in carbon emission coefficients and carbon trading prices do not reverse the performance ranking among different delivery modes. This demonstrates that the ranking conclusions of this study are robust within the tested parameter range. Parameter variations beyond this range are beyond the scope of this study and require further investigation.

The above simulation experiments not only verify the effectiveness of the collaborative delivery method but also demonstrate that the proposed system possesses advantages including flexible parameter configuration, rapid multi-scenario generation, and real-time visualization of results, indicating its natural potential for transformation into an educational tool.

6. Talent Development and Training

The performance characteristics, applicable scenarios, and representative models of intelligent delivery equipment such as UAVs and UGVs investigated in this project constitute important teaching contents for talent cultivation. The UAV-UGV collaborative delivery visualization simulation system developed in this study integrates equipment parameter configuration, path optimization, carbon emission calculation, and policy simulation functions, serving as an important auxiliary teaching platform for cultivating potential technical talents. Specifically, it can be applied in the following teaching activities.

6.1 Teaching on equipment selection analysis.

By adjusting key technical parameters of different UAV and UGV models (such as representative equipment including FP400 V4 and Ark ARK40), students can compare changes in delivery efficiency and carbon emissions under different conditions of payload capacity, speed, and endurance. This allows intuitive analysis of the influence of logistics equipment performance parameters on system operation effectiveness, deepens understanding of equipment selection principles and operational benefits, and cultivates the ability to conduct equipment selection based on data analysis.

6.2 Teaching on multi-objective optimization decision-making.

By adjusting multi-objective weight parameters such as delivery efficiency, safety, and low-carbon performance, students can observe the changes in collaborative delivery strategies in real time, understand the basic concepts of multi-objective coordination and trade-offs in logistics system optimization, and recognize that there is no absolutely optimal solution in logistics decision-making. Instead, the best comprehensive solution is achieved under different decision preferences and constraint conditions, thereby improving system analysis and decision-making capabilities.

6.3 Teaching on low-carbon policy simulation.

The system incorporates a carbon market policy simulation module, covering typical policy scenarios such as total carbon emission control, carbon emission intensity control, and the “dual-control” mechanism. It enables students to simulate and analyze changes in delivery routes, equipment configurations, and carbon emission levels under different policy constraints. This guides practitioners to understand the relationship between logistics equipment applications and system optimization under the national “dual-carbon” strategy, achieving an organic integration of logistics technology/equipment education and green logistics development concepts.

7. Conclusion

This study is conducted under the dual background of carbon emission dual-control policies and the development of the low-altitude economy. Focusing on the three practical constraints of efficiency, safety, and low-carbon development in urban last-mile logistics, this study establishes an air-ground collaborative delivery system combining UGV-based trunk transportation with UAV-based last-mile delivery. By incorporating a phased UAV energy consumption model, a dynamic carbon footprint accounting method is developed. Furthermore, a multi-objective optimization model considering delivery efficiency, transportation safety, total carbon emissions, and emission intensity is constructed. Based on HTML5, Canvas and Three.js dual rendering engines, an integrated visualization simulation and decision-support platform is developed.

The research demonstrates three major innovative contributions. First, at the model level, the study integrates the dynamic carbon footprint generated during UAV takeoff, cruising, hovering, and landing phases into the optimization framework, while simultaneously incorporating dual constraints of total carbon emissions and emission intensity. It establishes a three-dimensional optimization objective integrating efficiency, safety, and low-carbon performance, and distinguishes the differentiated obstacle avoidance mechanisms of air and ground equipment, addressing the limitations of traditional models with static carbon calculations and single-dimensional optimization objectives. Second, at the simulation platform level, the study adopts a dual-view synchronous rendering architecture combining two-dimensional and three-dimensional visualization, integrates carbon footprint heat maps and time-series visualization tracking modules, and introduces multiple carbon policy comparison simulation functions, enabling both algorithm validation and professional practical training. Third, at the mechanism analysis level, multiple random scenarios and multidimensional sensitivity experiments are conducted to verify the comprehensive advantages of total-emission and intensity dual-control carbon regulation and quantitatively reveal the long-term incentive effect of carbon trading prices on intelligent delivery equipment selection and route planning.

Multiple random simulation experiments fully demonstrate the comprehensive advantages of air-ground collaborative delivery. In the urban delivery scenario with a task density of 20 orders/100 km^2, the collaborative strategy significantly reduces delivery time and ground travel distance compared with traditional fuel-powered trucks while achieving substantial carbon emission reductions. The proposed building obstacle avoidance heuristic algorithm achieves a 100% obstacle avoidance success rate and a path length coefficient of variation of only 0.132 across 50 random test cases, demonstrating strong simulation platform stability. Sensitivity tests with ±20% variations in carbon emission coefficients and carbon trading prices confirm that the core conclusions regarding efficiency improvement and emission reduction advantages of collaborative delivery compared with single UAV delivery and traditional trucks remain unchanged.

From the perspective of educational application value, the proposed simulation platform integrates equipment parameter adjustment, multi-objective trade-off analysis, and carbon policy simulation functions. It can serve as a digital training platform for intelligent logistics education, helping learners intuitively understand air-ground unmanned delivery operations and low-carbon emission calculation methods, thereby providing strong support for cultivating practical talents in urban intelligent logistics. However, this study is limited to static urban delivery environments and does not consider dynamic disturbances such as extreme weather conditions, equipment failures, and multi-depot distribution scenarios. Future research can further extend the system by incorporating multi-agent collaboration and real-time dynamic replanning modules to improve adaptability to real-world logistics environments.

Conflict of Interest

The author declares that they have no conflicts of interest in this work.

Acknowledgement

This research was funded by: China Federation of Logistics and Purchasing, 2026CSLKT3-507; Guangdong Provincial Education Evaluation Association, BDPG25084; Guangdong Provincial Higher Education Innovation Project (Philosophy and Social Sciences), 2025WTSCX159; Special acknowledgement: the 'Logistics Technology and Equipment' Smart Course Project at Guangzhou Huali College.

Reference

Chu, L. Y., & Huang, X. T. (2026). Optimization of collaborative delivery between logistics vehicles and drones considering carbon emissions in mountainous areas. Computer Engineering and Applications, 1–17. https://link.cnki.net/urlid/11.2127.TP.20260605.1706.022 [Chinese journal]

Dorling, K., Heinrichs, J., Messier, G. G., & Magierowski, S. (2017). Vehicle routing problems for drone delivery. IEEE Transactions on Systems, Man, and Cybernetics: Systems, 47(1), 70–85.

Du, X. Q., Zhang, X. S., Xie, Y. H., et al. (2025). Can carbon emission trading promote energy conservation and emission reduction in enterprises? A quasi-natural experiment based on the pilot carbon emission trading policy. Journal of Management Science in China, 28(7), 22–38. https://doi.org/10.19920/j.cnki.jmsc.2025.07.002 [Chinese journal]

Geng, K. K., Cheng, X. L., Ding, P. B., et al. (2026). Review of the development status of key technologies for air-ground collaborative systems. Journal of Mechanical Engineering, 1–20. https://link.cnki.net/urlid/11.2187.th.20260205.1509.026 [Chinese journal]

Li, B., Liu, B., Chen, A. Q., et al. (2021). Carbon footprint calculation of fruits and vegetables based on cold chain logistics mode. Journal of Refrigeration, 42(2), 158–166. [Chinese journal]

Li, D. D., Shang, C. X., Huang, Q. Z., et al. (2026). Research on carbon emission trading mechanisms based on total amount and intensity dual control under the "dual carbon" goals. Journal of Industrial Engineering and Engineering Management, 40(2), 209–219. https://doi.org/10.13587/j.cnki.jieem.2026.02.015 [Chinese journal]

Liao, J., Xie, R. H., Tang, J., et al. (2019). Carbon footprint calculation and empirical study of the whole-process cold chain logistics for litchi products. Packaging Engineering, 40(3), 19–29. https://doi.org/10.19554/j.cnki.1001-3563.2019.03.004 [Chinese journal]

Liu, G. H., Wu, J. Z., You, L., et al. (2018). Construction and empirical analysis of carbon footprint model for cold chain logistics systems. Journal of Refrigeration, 39(4), 19–25. [Chinese journal]

Murray, C. C., & Chu, A. G. (2015). The flying sidekick traveling salesman problem: Optimization of drone-assisted parcel delivery. Transportation Research Part C: Emerging Technologies, 54, 86–109.

Ren, X. H., Wang, L., & Zou, X. T. (2020). Research on innovative models of urban instant delivery based on multiple factors. Commercial Economic Research, (11), 133–136. [Chinese journal]

Rodrigues, T. A., Patrikar, J., Oliveira, N. L., et al. (2021). Drone flight data reveal energy and greenhouse gas emissions savings for small package delivery. arXiv preprint arXiv:2111.11463.

Tu, Q., Cai, Y. Z., & Li, Z. D. (2026). How does carbon emission trading promote urban energy green transformation? Evidence from panel data of 282 cities in China. Soft Science, 1–14. https://link.cnki.net/urlid/51.1268.g3.20260616.1715.009 [Chinese journal]

Wang, F., Xu, H. F., & Wang, J. S. (2026). Air-ground collaborative delivery route optimization for multiple distribution centers. Journal of South China University of Technology (Natural Science Edition), 54(6), 42–53. [Chinese journal]

Wu, G. H., Mao, N., Xu, B. J., et al. (2023). A collaborative delivery method for multiple vehicles and multiple drones based on adaptive large neighborhood search algorithm. Control and Decision, 38(1), 201–210. https://doi.org/10.13195/j.kzyjc.2021.2268 [Chinese journal]

Xu, S. F., Fei, W. X., Li, H., et al. (2026). UAV-UGV air-ground collaborative path planning method based on three-stage optimization. Acta Aeronautica et Astronautica Sinica, 47(7), 245–266. [Chinese journal]

Zhang, L., Wei, Y. Q., & Jiang, L. (2026). The impact mechanism and policy optimization of carbon emission trading on urban green development. Urban Development Studies, 33(3), 103–110. [Chinese journal]

Zhang, R. P., & Pan, X. (2025). Construction of a collaborative pathway between carbon tax and carbon emission trading under the "dual carbon" goals. International Trade, (9), 27–37+48. https://doi.org/10.14114/j.cnki.itrade.2025.09.003 [Chinese journal]

Zou, C., Yang, Q., Li, J., et al. (2026). Towards sustainable urban logistics: Route optimization for collaborative UAV–UGV delivery systems under road network and energy constraints. Sustainability, 18(2), Article 1091.

How to Cite: Qiao, Y., Deng, X., Huang, X., Chen, W., Lin, Y., Luo, Z., Du, Y., Li, L., Shen, M. & Chen, X. (2026). Optimization of UAV–UGV Last-Mile Collaborative Delivery under Dynamic Carbon Footprint Constraints: Visual Simulation and Scenario Analysis of Coordinated Air–Ground Unmanned Delivery System. *Journal of Global Humanities and Social Sciences, 07*(4), 287-306. https://doi.org/10.61360/BoniGHSS262020520408